

DOI: 10.1002/cbic.201402368

A Fluorimetric Readout Reporting the Kinetics of Nucleotide-Induced Human Ribonucleotide Reductase Oligomerization

Yuan Fu,^[a] Hong-Yu Lin,^[a] Somsinee Wisitpitthaya,^[a] William A. Blessing,^[a] and Yimon Aye^{*[a, b]}

Human ribonucleotide reductase (hRNR) is a target of nucleotide chemotherapeutics in clinical use. The nucleotide-induced oligomeric regulation of hRNR subunit α is increasingly being recognized as an innate and drug-relevant mechanism for enzyme activity modulation. In the presence of negative feedback inhibitor dATP and leukemia drug clofarabine nucleotides, hRNR- α assembles into catalytically inert hexameric complexes, whereas nucleotide effectors that govern substrate specificity typically trigger α -dimerization. Currently, both knowledge of and tools to interrogate the oligomeric assembly pathway of

RNR in any species in real time are lacking. We therefore developed a fluorimetric assay that reliably reports on oligomeric state changes of α with high sensitivity. The oligomerization-directed fluorescence quenching of hRNR- α , covalently labeled with two fluorophores, allows for direct readout of hRNR dimeric and hexameric states. We applied the newly developed platform to reveal the timescales of α self-assembly, driven by the feedback regulator dATP. This information is currently unavailable, despite the pharmaceutical relevance of hRNR oligomeric regulation.

Introduction

Feedback modulation is a central regulatory component in cellular information relay and decision making.^[1] Aberrant processing of feedback circuits is often associated with disease phenotypes.^[1–3] As a central regulator of nucleotide metabolism, ribonucleotide reductase (RNR) is a key drug target enzyme operating under tight feedback regulation.^[4–9] Recent biophysical and structural studies have shown that the feedback regulation of RNR imposed by the metabolite dATP—a ubiquitous mechanism in RNRs from yeast, mice, and humans—is coordinated with nucleotide-induced oligomerization of the RNR large subunit α .^[8–14] However, neither the timescale of the self-assembly nor the identity of the transient intermediates involved in the assembly process have been interrogated in RNR from any species.

The human RNR (hRNR) holocomplex, composed of α and β subunits, catalyzes the rate-limiting conversion of nucleoside diphosphates (NDPs) to their deoxy forms (dNDPs) in the de novo biosynthesis pathway of dNTPs required for DNA replication and repair.^[4–9] hRNR activity is positively correlated with cancer cell growth, and suppressing hRNR activity is an effec-

tive strategy for repressing tumor survival, as demonstrated by a wealth of clinically used nucleoside antimetabolites.^[9,15,16] The catalytic activity and substrate specificity of hRNR are tightly regulated allosterically. This allosteric regulation occurs exclusively on the α subunit.^[6,8] ATP or dATP binding at the allosteric activity (A) site on α respectively stimulates or suppresses overall RNR enzymatic activity. dNTP/ATP binding at the allosteric specificity (S) site determines the substrate specificity of α .

Mounting evidence indicates that allosteric regulation is strongly coupled to nucleotide-induced oligomeric state changes that occur solely on hRNR- α and do not require β .^[8–14] The physiological relevance of such α oligomeric equilibria has also been demonstrated recently with the α -specific hexamerization-coupled inhibition induced by nucleotides of the anti-leukemic therapeutic clofarabine (ClF).^[12] With dNTP/ATP natural allosteric effectors, some disagreement exists about whether higher-order oligomers can be assessed.^[8–14] However, a large number of biochemical and structural reports have shown that the binding of the natural feedback allosteric inhibitor dATP at the A site induces α hexamerization of eukaryotic RNRs.^[8–12,14] In addition, nucleotide effector binding at the S site is believed to prime α to initiate substrate selection through α dimerization.^[6,8,10,11] The present study reports the development of the first readout directly reporting the two distinct hRNR- α oligomeric states. We applied this newly developed platform to monitor hRNR- α hexamerization events, triggered by the feedback regulator dATP, in real time (Figure 1).

[a] Dr. Y. Fu, Dr. H.-Y. Lin,[†] S. Wisitpitthaya,[†] W. A. Blessing, Prof. Y. Aye
Department of Chemistry and Chemical Biology, Cornell University
Ithaca, NY 14853 (USA)
E-mail: ya222@cornell.edu

[b] Prof. Y. Aye
Department of Biochemistry, Weill Cornell Medical College
New York, NY, 10065 (USA)

[†] These authors contributed equally to this work.

 Supporting information for this article is available on the WWW under <http://dx.doi.org/10.1002/cbic.201402368>.

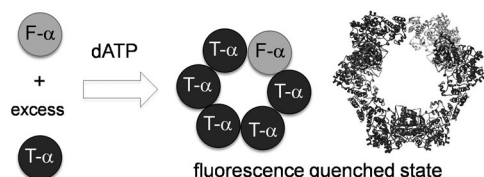


Figure 1. A fluorescence readout directly reporting RNR- α hexamerization. Feedback inhibitor dATP binding at the A site induces assembly of α_6 states in which the donor fluorescein signal is quenched. Gray and dark spheres are fluorescein (F)- and tetramethylrhodamine (T)-labeled α monomers. Hexamers of all T- α are omitted for clarity. The ribbon represents the known 6.6 Å crystal structure of dATP-bound α_6 from *S. cerevisiae* (3PAW).

Results and Discussion

Fluorescence assay development

We first focused on dATP-induced hexamerization as a readout, initially investigating the quenching of intrinsic tryptophan fluorescence as a hexamerization reporter.^[17] No fluorescence change was observed upon dATP-induced α oligomerization, presumably because of the large number of Trp residues (12) on α . We thus undertook identification of a robust fluorophore labeling method with minimal perturbation to α oligomerization. The functionality of hRNR- α depends on the presence of essential Cys residues in the reduced (free thiol) state.^[4] Some of these residues reside on the solvent-exposed flexible C-terminal tail of α . hRNR- α is also highly sensitive to oxidation, and the oxidized protein is prone to precipitation. These features rendered incompatible a number of site-specific chemical- and mutagenesis-based labeling strategies that have been used successfully with the bacterial RNRs. For instance, we found that the prolonged reaction time and additives used in native chemical ligation^[18] unavoidably led to protein precipitation.

Previous work showed that N-terminal hexahistidine (His₆)-tagged α hexamerizes in the presence of dATP or ClF di- and triphosphates [ClF(D)P] in the same manner as the enzyme from which the His₆ tag has been removed.^[11,12] We thus anticipated that a fluorophore could be incorporated site-specifically by using ATTO dyes^[19] that bind to the His₆ tag. However, because ATTO dye labeling of the His₆ tag is noncovalent, we observed dye dissociation under dilute reaction conditions. We also attempted to use a Lap tag,^[20] which can be enzymatically modified, inducing covalent labeling of the Lap-tagged protein. However, the N-terminal Lap-tagged α failed to hexamerize upon treatment with hexamerization inducers. We also constructed and isolated catalytically functional α variants genetically encoded at the N-terminus with the commonly used protein tags: enhanced green fluorescent protein (eGFP),^[21] monomeric red fluorescent protein (mRFP),^[22] and HaloTag.^[23] These fusion proteins also impeded hexamerization. Our labeling efforts highlighted the sensitivity of hRNR- α hexamerization to N-terminal perturbations, an observation consistent with the fact that the N-terminus provides the physical dimer interface within the trimer-of-dimers (α_2)₃ complex.^[10,12]

We ultimately identified a non-intrusive labeling strategy by using small amounts of thiol-reactive dyes in the presence of

the reducing agent dithiothreitol (DTT). We hypothesized that the presence of the reducing agent provided a reaction environment in which DTT maintained the solubility and functional integrity—specifically, the oligomerization capacity—of hRNR- α . A 20 min incubation with either 5-iodoacetamidofluorescein (5-IAF), or tetramethylrhodamine-5-iodoacetamide dihydroiodide (5-TMRIA), resulted in 1.0 ± 0.2 and 0.9 ± 0.1 equiv, respectively, of covalent fluorophore labeling per polypeptide (Figure 2A and B and Table S1). Liquid chromatography tandem

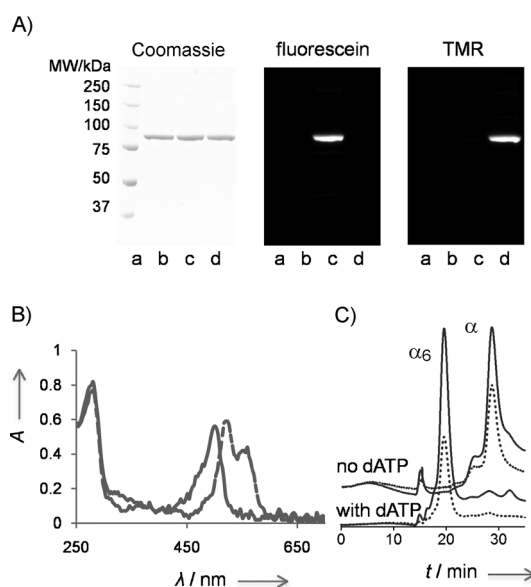


Figure 2. The covalent fluorophore labeling strategy is non-intrusive to α oligomerization. A) In-gel fluorescence analysis by denaturing SDS-PAGE validates covalent fluorophore labeling. Lanes a–d: ladder, unlabeled- α treated under otherwise identical conditions, F- α , T- α . B) Absorbance spectra overlay of F- α (—) and T- α (---) (see also Table S1 and Figure S1). Note: peak splitting is a common spectral feature of TMR-labeled proteins (see, e.g., manuals from Life Technologies, Genaxxon BioScience, and AnaSpec). C) Labeled protein hexamerizes efficiently. Gel filtration analysis of F- α with and without dATP. ----- and designate A280 and A495 traces, respectively (see also Figure S2).

mass spectrometry (LC-MS/MS) analysis suggested that, based on 66% peptide coverage, labeling occurred primarily on three solvent-exposed catalytically non-essential Cys residues: Cys254, Cys662, and Cys779 (Figure S1). Importantly, gel filtration analysis showed that both the fluorescein-labeled and the tetramethylrhodamine-labeled α (hereafter F- α and T- α) hexamerized as efficiently as unlabeled α in the presence of 20 μ M dATP in the running buffer (Figures 2C and S2). The activities of F- and T- α were not largely perturbed, maintaining $72 \pm 2\%$ and $68 \pm 8\%$, respectively, of the activity of unlabeled α treated under otherwise identical conditions (Figure S3A). The capability of the labeled α to undergo α hexamerization suggests that our covalent labeling strategy was noninvasive and therefore suitable for modeling the hexamerization pathway. However, the observed partial loss in activity of the labeled α means that the calculated rates of oligomerization might differ slightly from those of the unlabeled protein. We further validated the

capacity of the labeled proteins to hexamerize by using the known hexamerization inducers CIFD(T)P (Figure S2).

We next sought to identify the simplest and most reliable fluorimetric readout of α hexamerization. Fluorescent quenching in the presence of a 1:5 mixture of F- α (donor) and T- α (acceptor) was the most versatile and sensitive hexamerization reporter (Figure 1). Under these conditions, saturating concentrations of all three hexamerization-inducers—dATP and CIFD(T)P—caused a 46–48% drop in F intensity. Titration with dATP revealed a dose-dependent signal drop (Figure 3 and

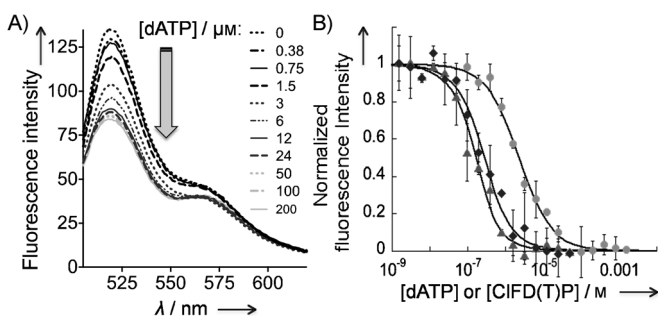


Figure 3. Fluorescence quenching is coupled to wt- α hexamerization. A) Emission spectra of 1:5 F-T- α (0.2 μ M) with increasing dATP concentrations (0–200 μ M). B) Dose-dependent fluorescence quenching promoted by α hexamerization inducers: dATP (●), CIFDP (◆), and CIFTP (▲). Standard deviation was derived from $N=3$. Normalized intensity of 1.0 was set for the largest magnitude of drop in fluorescence intensity at the saturating concentrations of respective inducers and corresponded to a 46–48% drop in F intensity at 520 nm (see also Figure S4 and S5).

S4A). The half-maximal effective concentration (EC_{50}) of the dATP-driven α hexamerization was calculated to be $2.3 \pm 0.3 \mu$ M (Figure 3B). Similar titrations with CIFD(T)P showed that α hexamerization was inducible at a concentration much lower than that of dATP (Figure 3B). Because the minimum protein concentration for reliable fluorescence readout was ~ 180 nM, we fit the CIFD(T)P titration data to a tight-binding equation,^[24] yielding K_d values instead of EC_{50} values. The resultant K_d values of $\sim 185 \pm 36$ and 74 ± 19 nM, respectively, were within the range of the K_i values deduced from inhibition assays.^[11]

Importantly, nucleotides such as substrate CDP and the clinically used substrate analogue suicide inactivator, gemcitabine diphosphate (F2CDP), which are incapable of altering the hRNR- α subunit quaternary structure,^[9] did not induce an appreciable fluorescence change (Figure S5A and S5B). Controls in which F- α alone or unlabeled α in place of T- α (Figure S5C–D) was treated with inducers showed a < 1 –3% drop in donor intensity. These observations suggest that no fluorescein quenching occurred due to nucleotide binding or interaction with protein residues.

To confirm that the observed quenching was due to a fluorescence resonance energy transfer (FRET) process, we subtracted the donor fluorescein intensities obtained from the samples with F- α alone from the emission spectra of an F- and T- α mixture at 0 and 200 μ M dATP. An increase in T- α -specific intensity promoted by dATP was observed, indicating the presence of FRET (Figure S4B and C).

hRNR- α is monomeric in the absence of any substrates and effectors,^[8–14] and a wealth of evidence indicates that α alone can adopt a dimeric state. The α_2 dimeric state is induced upon effector binding at the S site,^[6,8–14] and dimerization is a prerequisite for adoption of the $\alpha_2\beta_2$ active state by the holoenzyme.^[25] The α_2 quaternary state of hRNR- α (without β) has also been well-characterized by crystallography.^[10] We were thus interested in the extent to which our fluorescence protocol could distinguish between α hexamerization and dimerization. We first took advantage of the previously characterized hRNR His₆-D57N- α .^[11] D57N- α is unresponsive to dATP-induced hexamerization-coupled inhibition. However, owing to dATP binding at the S site, this mutant is dimeric under saturating concentrations of dATP.^[11,26] His₆-D57N- α was covalently labeled with either F or T (Figure S6A), resulting in 0.9 ± 0.11 and 0.9 ± 0.3 equivalents, respectively, of covalent dye labeling per polypeptide (Table S1 and Figure S6B). Gel filtration analysis in the presence of dATP in the running buffer showed that the labeled proteins dimerized with efficiencies similar to that of the unlabeled mutant (Figure S2E and S2I). The specific activities of F- and T-D57N- α were $73 \pm 8\%$ and $61 \pm 2\%$ of the unlabeled D57N- α (Figure S3A).

Compared with the 46–48% drop in F intensity observed for dATP-induced wild-type (wt)- α hexamerization, dATP promoted $37 \pm 3\%$ quenching when wt- α was replaced with mutant α under otherwise identical conditions. As a means for identifying a set of conditions in which the magnitudes of quenching resulting from dimerization and hexamerization are optimally different, the drop in the donor intensity at 520 nm was examined across various donor:acceptor ratios of F-T-D57N- α (dimerization) and compared with the results obtained for F-T- α (hexamerization; Figure S3B). The results showed that the fluorimetry sensitivity enabled the extent of quenching induced by α dimerization to be $10 \pm 3\%$ lower than for α hexamerization. Notably, the degree of donor quenching gradually declined as the proportion of T- α with respect to F- α decreased. This observation additionally corroborated the presence of FRET (Figure S4B and C). As the ratio of F-T- α decreased beyond 1:1, the degree of quenching reached a plateau. A similar saturation effect was reported in previous FRET studies in which changes in the relative populations of donors to acceptors have little effect on FRET efficiency when the donor/acceptor ratio is < 1 .^[27]

The allosteric activator ATP is also thought to induce α oligomerization independent of β , although the precise nature of the resulting oligomeric state remains unsettled.^[8–14] However, initial attempts to examine the effects of ATP by using our new fluorescence assay revealed that the high (millimolar) ATP nucleotide concentrations required to induce α oligomerization quenched the fluorescein signal, even in the sample containing only F- α alone or in the presence of 5-IAF dye alone without α . Thus, the effects of ATP cannot be analyzed by this assay.

Stopped-flow fluorescence analyses

The successful development of a direct and sensitive fluorescence readout of the dATP inhibitor-induced α oligomerization

gave us an impetus to study the kinetics of the dATP-driven hexamerization as a starting point. hRNR homo-oligomerization is an area of great pharmaceutical interest,^[9–12] and its relevance has been biochemically proven with both the isolated enzyme^[8–11,13,14] and the functional hRNR- α ectopically expressed in cells.^[12] However, the mechanism and kinetics of the individual steps in the pathway remain unmapped in RNR from any species. The results of discontinuous inhibition assays and electron microscopy studies have inferred only an upper limit (3–4 min).^[11,12]

In a FRET-based mixing assay using a fluorescence stopped-flow device, we first tested the conditions that permitted only dimerization—namely, dATP-induced D57N- α dimerization.^[10,26] Total fluorescence at wavelengths of > 505 nm was monitored after the rapid mixing of a 1:5 solution of F:T-D57N- α from one syringe and 200 μM dATP from another (Figure S7 A). The process was surprisingly slow, requiring measurements longer than 180 s. The hyperbolic trace fit a second-order dimerization rate law:

$$I(t) = \frac{I_0 - I_\infty}{1 + 2[\alpha]_0 kt} + I_\infty \quad (1)$$

where $I(t)$, I_0 and I_∞ designate the fluorescence intensity at time t , time zero, and infinite time, respectively, and $[\alpha]_0$ is the initial concentration of D57N- α monomer (Figure S7 A). The derivation of this equation is shown in the Supporting Information. Three lines of evidence further supported the second-order nature of the process: 1) The rate was dependent on protein concentration (Figure 4A); the apparent rate constant, k_{app} [i.e., $2[\alpha]_0 k$ in Eq. (1)], was a linear function of $[\alpha]_0$ (Figure 4B). 2) Provided that dATP was present in saturating concentrations, changing dATP concentration had little or no effect on the rate (Figure S7 B), implying that dATP binding was rapid under these conditions. 3) A plot of the rate of total fluorescence intensity drop $[dI(t)/dt]$ versus $[I(t)]^2$ was also linear, further confirming the second-order nature of the kinetic process (Figure 4C). The data revealed that D57N- α dimerization induced by dATP binding at the S site occurs with a bimolecular rate constant of $(5.8 \pm 0.2) \times 10^4 \text{ M}^{-1} \text{ s}^{-1}$. Although in our hands, D57N- α was observed to be a dimer at 100 μM dATP,^[11,12] high dATP concentrations have been implicated to induce further oligomerization of the mutant.^[13] The bimolecular rate constant derived above was thus unambiguously verified by replicating the experiments at low dATP concentrations in which the mutant was undisputedly a dimer (Figure S8). The dimerization rate constants were found to be largely unaltered: $[(5.0 \pm 0.4) \times 10^4]$ and $[(5.9 \pm 0.4) \times 10^4] \text{ M}^{-1} \text{ s}^{-1}$ at 20 and 33 μM dATP, respectively.

We also probed whether the α dimerization rate was influenced by the identity of the nucleotide effector. We thus opted to exploit an dGTP allosteric effector that binds exclusively at the S site and induces wt- α dimerization.^[6,8–11] We first confirmed under steady-state conditions that the addition of saturating amounts of dGTP (0.1 mM) to a 1:5 mixture of F:T-wt- α promoted a 30–35% percentage drop in F- α intensity, a value within the range observed for dATP-induced D57N- α di-

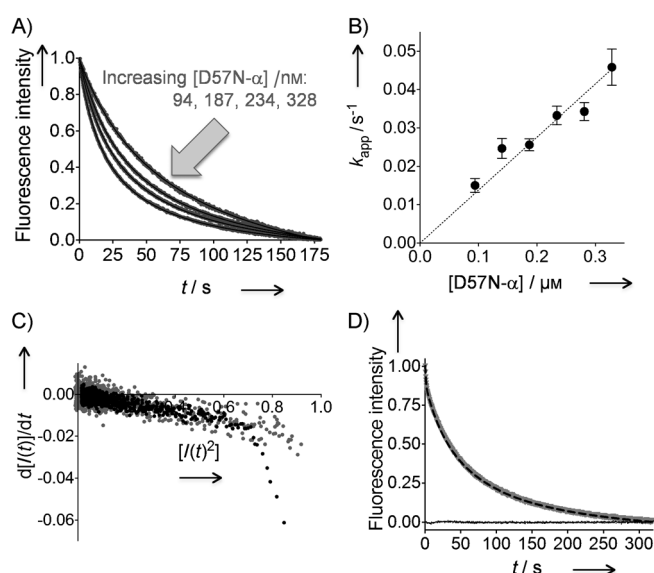


Figure 4. Stopped-flow fluorescence measurements of 100 μM dATP-induced α dimerization and hexamerization. Each trace is an average of ≥ 9 independent traces. A) D57N- α dimerization rate as a function of mutant protein concentration. Averaged kinetic traces from representative concentrations are shown. Solid lines indicate fit to Equation (1) (see also Figure S7 and S8). The observed k_{app} is linearly dependent on the mutant protein concentration; $k_{\text{app}} = 2[\alpha]_0 k$ in Equation (1). C) A plot of $d[I(t)]/dt$ against $[I(t)]^2$ overlaying the data from D57N- (gray) and wt- (dark) α . D) Kinetic trace for dATP-promoted wt- α hexamerization measured over 300 s (gray curve). The black dashed curve and baseline traces indicate the fit to the data using Berkeley Madonna [Eq. (2)] and residuals, respectively (see also Figure 5).

merization (Figure S9 A). The subsequent stopped-flow monitoring of dGTP-induced wt- α dimerization revealed a kinetic trace that best fit the dimerization rate equation [Eq. (1)]. The analysis provided a second-order rate constant of $(7.7 \pm 0.6) \times 10^4 \text{ M}^{-1} \text{ s}^{-1}$ (Figure S9 B). Although substrate specificity was conferred by specific effector binding at the S site—dGTP binding selecting ADP substrate and dATP binding selecting UDP substrate^[6,8–10]—our data suggest that the two different effectors induced α dimerization at nearly identical rates.

We then probed α hexamerization with stopped-flow mixing of the wt protein and the feedback inhibitor dATP. The altered oligomeric state of mammalian α in the presence of the natural inhibitor dATP has been investigated by using various biophysical methods.^[8–14] Gel filtration,^[10,11,14] dynamic light scattering^[10,13] and gas-phase electrophoretic molecular mobility^[14] analyses have collectively established that dATP binding to the A site drives mammalian RNR- α hexamerization. X-ray crystallography and electron microscopy data from 6.6 Å dATP-bound *Saccharomyces cerevisiae* RNR- α hexamers^[10] and CIF nucleotides-induced hRNR hexamers,^[12] respectively, have also provided structural insights into the inhibited complexes that adopt the trimer-of-dimers assembly. In the present study, we sought to construct the missing kinetic model of dATP-assisted eukaryotic RNR- α hexamerization exemplified by the human enzyme.

D57N- α was replaced with wt- α under the stopped-flow conditions described above (Figure 4D). The resulting kinetic

trace was identical to that obtained from the stopped-flow mixing of D57N- α and dATP, except in the early period, which featured an additional fast phase. Consistent with this observation, initial fitting of this trace to the dimerization equation showed a deviation from the fit within the < 10 s period. Conversion of this kinetic trace to a plot of the rate of total fluorescence intensity drop (Figure 4C) revealed that, unlike the trace obtained for dATP-induced D57N- α dimerization, that of the dATP-induced wt- α hexamerization deviated clearly from linearity. The overall time course of dATP-induced wt- α hexamerization was best fit to a two-step kinetic model by using the Berkeley Madonna program (v 8.3.18) [Figures 4D and 5, Eqs. (2.1)–(2.4)]. The fast phase fit well to a monoexponential rate law with a rate constant of 1.3 ± 0.2 s $^{-1}$. Interestingly, the fitted second rate constant belonging to the slow phase of the FRET change in wt- α , $(6.9 \pm 0.6) \times 10^4$ M $^{-1}$ s $^{-1}$, was very close to the dimerization rate constant for D57N- α determined above: $(5.8 \pm 0.2) \times 10^4$ M $^{-1}$ s $^{-1}$. This unexpected finding suggested that the slow phase is associated with dimerization.

We used Equations (2.1)–(2.4) to model the observed kinetic trace as a two-step sequence: $\alpha \rightarrow \alpha^* \rightarrow (\alpha^*)_2$, in which α^* was postulated to be α with an altered conformation. Steps subsequent to the rate-determining dimerization did not affect the kinetic trace or the derivation of Equation (2.4) (see the Supporting Information for more details):

$$d[\alpha]/dt = -k_1 [\alpha] \quad (2.1)$$

$$d[\alpha^*]/dt = k_1 [\alpha] - 2k_2 [\alpha^*]^2 \quad (2.2)$$

$$d[(\alpha^*)_2]/dt = k_2 [\alpha^*]^2 \quad (2.3)$$

$$I(t) = I_0 - U[\alpha^*] - V[(\alpha^*)_2] \quad (2.4)$$

In Equations (2.1)–(2.4), α^* represents an intermediate formed during the fast phase, $(\alpha^*)_2$ is a dimer that can undergo further oligomerization at a rate(s) faster than that of $(\alpha^*)_2$ formation, k_1 and k_2 are the rate constants of the two steps, $I(t)$ and I_0 designate the measured fluorescence intensity at time t and time zero, respectively, and U and V are constants. Figure 5A and B shows a kinetic simulation of this model using the Berkeley Madonna software. To test the hypothesis that $\alpha \rightarrow \alpha^*$ conversion was associated with conformational transition, we evaluated the effects of various protein concentrations (Figure 5C). As expected, a large part of each of the resultant traces representing the rate-determining dimerization step was affected by protein concentration. Extraction of the rate constants (Table S2) by fitting the averaged traces at each α concentration to Equations (2.1)–(2.4) revealed that the fast phase preceding dimerization was a unimolecular process independent of protein concentration (Figure S10). By contrast, excluding the initial 10 s period from each trace and approximating the remaining part to dimerization [Eq. (1)] showed that the apparent rate constants for the slow step changed linearly as a function of α concentration (Figure S10).

These data unexpectedly revealed that α dimerization is the rate-determining step in dATP-promoted wt- α hexamerization, but subsequent faster step(s) were not revealed. The fast step

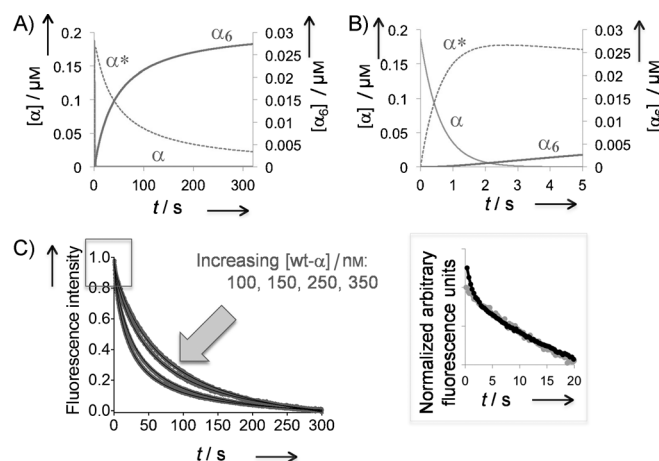


Figure 5. Kinetics of 100 μ M dATP-induced wt- α hexamerization. A) Kinetic simulation for the overall hexamerization process. B) Initial period of simulation in (A). Simulations were carried out with Berkeley Madonna software (v 8.3.18); the rate constants were derived from fitting the averaged kinetic trace in Figure 4C to Equations (2.1)–(2.4) (see text and Supporting Information). Note that $(\alpha^*)_2$ did not accumulate but was rapidly converted to α_6 at a rate faster than that of rate-determining $(\alpha^*)_2$ formation. The experimental kinetic trace (Figure 4D) and Equations (2.1)–(2.4) thus exclude information on the fast steps beyond the rate-determining step. C) Representative averaged kinetic traces at various wt- α concentrations (see also Table S2 and Figure S9). Inset at right is the expansion of the initial period at $[\alpha] = 0.2$ μ M (dark trace) overlaid with the corresponding trace for D57N- α (0.2 μ M) (gray trace) after normalization.

relating to the proposed conformationally altered α^* was notably absent in the wt- α dimerization triggered by dGTP binding at the S site, as well as in D57N- α dimerization in which dATP only associates with the S site under the given conditions. We thus posit that the rapid conformational transition of α to α^* (< 10 s), unique to wt- α , is linked to dATP-binding at the A site, effectively giving rise to a dimer primed specifically to proceed ultimately to formation of the hexameric (α_6) state. As this priming step was absent in D57N- α with dATP and in wt- α with dGTP bound at the S site (Figure 4A–C, 5C inset, S7–9), dATP binding at the A site on wt- α likely enables allosteric adjustments through conformational transitioning at an early step that precedes dimerization.

The rate-determining nature of the dimerization limited our ability to obtain a readout of the kinetics of the remaining steps representing the $\alpha_2 \rightarrow \alpha_6$ transition. Because termolecular events in which the three α_2 dimers simultaneously assemble into a hexamer are statistically improbable, the α_4 state is likely a transient intermediate along this pathway. As the rate constants of dGTP-induced wt- α dimerization and dATP-induced D57N- α dimerization are similar, the dGTP-bound (wt- α) $_2$ dimer is considered a reasonable dimeric precursor with a vacant A site to accept dATP, thereby proceeding along the $\alpha_2 \rightarrow \alpha_6$ trajectory. Thus to approximate the kinetics of the $\alpha_2 \rightarrow \alpha_6$ oligomeric transition, we performed stopped-flow mixing of one syringe containing wt- α pre-incubated with 0.1 mM dGTP and another containing 200 μ M dATP (Figure 6A). Although the overall trace did not fit to simple rate laws, the initial period (~ 50 s) fit well to the second-order dimerization equation [Eq. (1)] (Figure 6B). This initial period presumably reports the

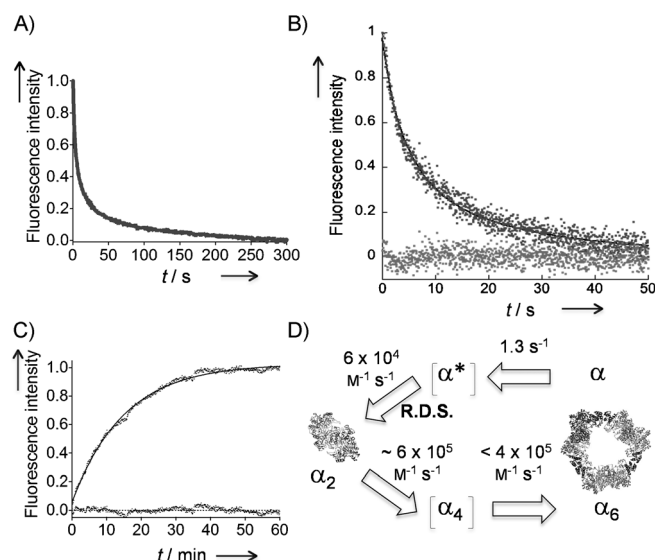


Figure 6. A–C) Estimating the rates of $\alpha_2 \rightarrow \alpha_6$ and $\alpha_2 \rightarrow \alpha$ transitions in saturating dATP. A) Averaged kinetic trace ($N=9$) resulting from mixing dATP and wt- α presaturated with dGTP at the S site (see also Figure S10 A). B) The first 50 s of a representative kinetic trace from (A). Solid black line indicates the fit to Equation (1). Baseline trace indicates residuals (see also Figure S10 B). C) Fluorescence recovery after 1:1 (v/v) mixing of 2 μM unlabelled D57N- α dimers (in 200 μM dATP) and 375 nm labeled D57N- α dimers (1:1 mixture of F:T-D57N- α in 200 μM dATP). Solid line shows monoexponential fit. Residuals are shown at the baseline. D) Oligomerization model in the presence of saturating dATP. The reverse process is considered negligible in the presence of saturating dATP and was $1.1 \times 10^{-3} \text{ s}^{-1}$ for $\alpha_2 \rightarrow \alpha$. Dimerization was the rate-determining step (R.D.S.) and was estimated to be one order of magnitude slower than subsequent oligomerization steps. α^* is the proposed conformationally altered transient state of α that can ultimately undergo α hexamerization process, as described in the text. The tetrameric state is proposed as a transient intermediate because α_2 trimerization directly to α_6 in a single step is considered to be an unlikely event. Ribbon depictions for α_2 and α_6 are based on the known crystal structures of hRNR- α (2WGH) and yeast RNR- α (3PAW), respectively. Each α monomer is shown in dark and light gray, and the N-terminal domain housing the A site is shown in black. See the Table of Contents for a color figure.

bimolecular combination of α_2 and α_2 , affording a tetrameric intermediate. Concentration-dependent studies (Figure S11) showed that the apparent rate constant, $k_{\text{app}} [2[\alpha_2]_0 k$ in Eq. (1)] is linearly dependent on $[\alpha_2]$, yielding a rate constant of $(5.6 \pm 0.2) \times 10^5 \text{ M}^{-1} \text{ s}^{-1}$. The fact that the rate constant for $\alpha_2 \rightarrow \alpha_6$ conversion was an order of magnitude faster than that for the rate-determining dimerization ($\sim 6 \times 10^4 \text{ M}^{-1} \text{ s}^{-1}$) was in line with our expectations. These observations further reinforced the previous findings that the new fluorescence platform can differentiate the initial dimerization event from the subsequent formation of higher-order α oligomers.

Because of the known stability of the α_2 and α_6 states in the presence of appropriate effectors under saturating concentrations,^[8–14] we were interested to probe the dissociation rate under the same experimental conditions, in addition to the rate of association. As an initial step, the propensity of dimer decomplexation was examined by using dATP-bound D57N- α dimers. Addition of a large excess of unlabeled D57N- α dimer to a sample containing labeled dimer resulted in a slow (~ 1 h) recovery of donor intensity at 520 nm (Figure 6C). A mono-

exponential fit to the data gave a first-order rate constant of $(1.1 \pm 0.2) \times 10^{-3} \text{ s}^{-1}$ for the subunit exchange process, which is equivalent to the dimer dissociation rate constant^[28] in the presence of saturating concentrations of dATP. From α_2 association and dissociation events, the dimer–monomer equilibrium constant in the presence of saturating concentrations of dATP was calculated to be 18 nM. In the absence of any nucleotide, the equilibrium constant for the dimer–monomer transition has been reported to be 170 μM .^[29]

Conclusions

We have developed a simple readout that can directly report hRNR- α oligomerization events with high sensitivity. The pre-steady-state kinetic analyses with this newly developed platform revealed that: 1) hRNR oligomerization is a slow process; 2) dimerization is the unexpected rate-limiting step along the dATP-induced hexamerization-coupled inhibition pathway (Figure 6D); 3) the rates of dimerization in response to nucleotide binding at the allosteric specificity (S) site are similar for dGTP and dATP, likely suggesting that substrate selection is not governed by kinetics but through the binding equilibrium; 4) the dissociation of dimer is very slow, implying that the complex, once formed, is tight in the presence of saturating concentrations of dATP; and 5) kinetics of the subsequent steps beyond the rate-determining dimerization were estimated to be an order of magnitude faster. In this model, the reverse process is considered negligible in the presence of saturating concentrations of dATP.

dATP is the only endogenous ligand capable of downregulating RNR activity.^[5,6,8,9,30] Thus, feedback regulation is essential in maintaining dNTP pools at appropriate levels and sustaining DNA replication fidelity.^[9,30] Our initial data provide a starting point for understanding oligomeric regulatory kinetics in response to an important feedback inhibitor. Analogous measurements of CIFD(T)P-induced α hexamerization will be the subjects of future studies. Our fluorimetric platform also paves the way toward rapid identification of non-nucleotide-based small molecules that can bind and promote self-assembly of α . Such molecules could have the potential to inhibit hRNR.

Experimental Section

See the Supporting Information (Tables S1–S2 and Figures S1–S11) for complete experimental methods.

Acknowledgements

We thank Professor Peng Chen for scientific discussions, Professor JoAnne Stubbe for scientific feedback, and the laboratories of Professors Peng Chen, Steven E. Ealick, and Hening Lin for use of the fluorimeter, inert atmosphere chamber, and LCMS instruments, respectively. We thank Professor Charles Richardson (Harvard Medical School) for the plasmid encoding E. coli TrxA. We acknowledge Dr. Sheng Zhang and the staff of the proteomics

and mass spectrometry facility at Cornell for LC-MS/MS technical support and the protein production facility at Cornell for the use of the stopped-flow spectrofluorimeter. ESR data were collected at the National Biomedical Research Center for Advanced ESR Technology (ACERT) at Cornell University, supported by NIH/NIGMS grant P41M103721 [Professor Jack Freed (PI); we thank Dr. Boris Dzikovski for his assistance]. This research was supported by a Hill Undergraduate Research Fellowship (to W.B.), a King Bhumbol Adulyadej Graduate Fellowship (to S.W.), and Cornell University junior faculty start-up funds, the Milstein Sesquicentennial Fellowship, the Affinito-Stewart grant from the President's Council of Cornell Women, a faculty development grant from the ACCEL program supported by NSF [SBE-0547373, Kent Fuchs (PI)], and the Arnold and Mabel Beckman Foundation through a Beckman Young Investigator award (to Y.A.).

Keywords: feedback inhibition · fluorescence reporter assay · human ribonucleotide reductase · oligomeric regulation · stopped-flow kinetics

- [1] M. Freeman, *Nature* **2000**, *408*, 313.
[2] K. Sneppen, S. Krishna, S. Semsey, *Annu. Rev. Biophys.* **2010**, *39*, 43.
[3] M. Csete, J. Doyle, *Trends Biotechnol.* **2004**, *22*, 446.
[4] J. Stubbe, W. van der Donk, *Chem. Rev.* **1998**, *98*, 705.
[5] L. Thelander, *Nat. Genet.* **2007**, *39*, 703.
[6] P. Nordlund, P. Reichard, *Annu. Rev. Biochem.* **2006**, *75*, 681.
[7] J. Shao, B. Zhou, B. Chu, Y. Yen, *Curr. Cancer Drug Targets* **2006**, *6*, 409.
[8] A. Hofer, M. Crona, D. T. Logan, B. M. Sjoberg, *Crit. Rev. Biochem. Mol. Biol.* **2012**, *47*, 50.
[9] Y. Aye, M. Li, M. J. C. Long, R. S. Weiss, *Oncogene* **2014**; DOI: 10.1038/onc.2014.155.
[10] J. W. Fairman, S. R. Wijerathna, M. F. Ahmad, H. Xu, R. Nakano, S. Jha, J. Prendergast, R. M. Welin, S. Flodin, A. Roos, P. Nordlund, Z. Li, T. Walz, C. G. Dealwis, *Nat. Struct. Mol. Biol.* **2011**, *18*, 316.
[11] Y. Aye, J. Stubbe, *Proc. Natl. Acad. Sci. USA* **2011**, *108*, 9815.
[12] Y. Aye, E. J. Brignole, M. J. C. Long, J. Chittuluru, C. L. Drennan, F. J. Asturias, J. Stubbe, *Chem. Biol.* **2012**, *19*, 799.
[13] O. B. Kashlan, B. S. Cooperman, *Biochemistry* **2003**, *42*, 1696.
[14] R. Rofougaran, M. Vodnala, A. Hofer, *J. Biol. Chem.* **2006**, *281*, 27705.
[15] P. L. Bonate, L. Arthaud, W. R. Cantrell, Jr., K. Stephenson, J. A. Secrist III, S. Weitman, *Nat. Rev. Drug Discovery* **2006**, *5*, 855.
[16] L. W. Hertel, G. B. Boder, J. S. Kroin, S. M. Rinzl, G. A. Poore, G. C. Todd, G. B. Grindey, *Cancer Res.* **1990**, *50*, 4417.
[17] J. R. Lakowicz in *Principles of Fluorescence Spectroscopy*, 3rd ed Springer, New York, **2006**.
[18] E. C. B. Johnson, S. B. H. Kent, *J. Am. Chem. Soc.* **2006**, *128*, 6640.
[19] E. G. Guignet, R. Hovius, H. Vogel, *Nat. Biotechnol.* **2004**, *22*, 440.
[20] C. Uttamapinant, M. I. Sanchez, D. S. Liu, J. Z. Yao, A. Y. Ting, *Nat. Protoc.* **2013**, *8*, 1620.
[21] R. Y. Tsien, *Annu. Rev. Biochem.* **1998**, *67*, 509.
[22] R. E. Campbell, O. Tour, A. E. Palmer, P. A. Steinbach, G. S. Baird, D. A. Zacharias, R. Y. Tsien, *Proc. Natl. Acad. Sci. USA* **2002**, *99*, 7877.
[23] G. V. Los, L. P. Encell, M. G. McDougall, D. D. Hartzell, N. Karassina, C. Zimprich, M. G. Wood, R. Learish, R. F. Ohana, M. Urh, D. Simpson, J. Mendez, K. Zimmerman, P. Otto, G. Vidugiris, J. Zhu, A. Darzins, D. H. Klaubert, R. F. Bulleit, K. V. Wood, *ACS Chem. Biol.* **2008**, *3*, 373.
[24] P. Kuzmič, S. Sideris, L. M. Cregar, K. C. Elrod, K. D. Rice, J. W. Janc, *Anal. Biochem.* **2000**, *281*, 62.
[25] E. C. Minnihan, N. Ando, E. J. Brignole, L. Olshansky, J. Chittuluru, F. J. Asturias, C. L. Drennan, D. G. Nocera, J. Stubbe, *Proc. Natl. Acad. Sci. USA* **2013**, *110*, 3835.
[26] Y. Fu, M. J. Long, M. Rigney, S. Parvez, W. A. Blessing, Y. Aye, *Biochemistry* **2013**, *52*, 7050.
[27] C. Berney, G. Danuser, *Biophys. J.* **2003**, *84*, 3992.
[28] C. Pan, *PLoS One* **2011**, *6*, e28827.
[29] C. P. Scott, O. B. Kashlan, B. S. Cooperman, *Biochemistry* **2001**, *40*, 1651.
[30] B. B. Zhou, S. J. Elledge, *Nature* **2000**, *408*, 433.

Received: July 9, 2014

Published online on September 24, 2014